The Plant Cell, Vol. 7, 43–55, January 1995 © 1995 American Society of Plant Physiologists

Transient Induction of a Peroxidase Gene in *Medicago truncatula* Precedes Infection by *Rhizobium meliloti*

Douglas Cook,[a,1] Dale Dreyer,[b] Dominique Bonnet,[a] Mary Howell,[a] Emmanuel Nony,[a] and Kathryn VandenBosch [b]

[a] Department of Plant Pathology and Microbiology, Texas A & M University, College Station, Texas 77843
[b] Department of Biology, Texas A & M University, College Station, Texas 77843

Although key determinative events of the *Rhizobium*–legume symbiosis are likely to precede bacterial infection, no plant genes have been identified that are expressed strongly prior to infection and nodule morphogenesis. A subtractive hybridization–polymerase chain reaction technique was used to enrich for genes induced during the early phases of the *R. meliloti–Medicago truncatula* symbiosis. One gene so identified encodes a putative plant peroxidase protein, which we have named Rip1 for *Rhizobium*-induced peroxidase. The accumulation of *rip1* transcript was rapidly and transiently induced by *R. meliloti* and by the corresponding lipooligosaccharide signal molecule Nod factor RmIV, which was both necessary and sufficient for *rip1* induction. The duration of maximal *rip1* expression coincided with the preinfection period: transcript levels for *rip1* were near maximal by 3 hr postinoculation and declined by 48 hr, coincident with early infection events and the onset of nodule morphogenesis. Furthermore, although *rip1* induction preceded bacterial infection by at least 24 hr, the transcript was localized to epidermal cells in the differentiating root zone that was subsequently infected by *Rhizobium*. Thus, a defining feature of the *Rhizobium* infection court is the prior induction of *rip1* expression.

INTRODUCTION

After inoculation with compatible rhizobia, certain leguminous plants are induced to form a unique organ on their roots, the nodule, where the plant provides conditions necessary for bacterial conversion of atmospheric dinitrogen to ammonia. Specificity in the *Rhizobium*–legume symbiosis is for compatibility, which is manifest by successful infection and nodule morphogenesis. Compatibility is first determined by preinfection events involving an exchange of molecular signals between the plant and the bacterium, which mediate their mutual differentiation (Fisher and Long, 1992). Flavonoids excreted by the plant root induce the expression of bacterial *nod* genes, whose function is required for nodulation and synthesis of a bacterial signal molecule, a lipooligosaccharide called Nod factor. The biological specificity of Nod factor is determined by chemical substituents on a common *N*-acetylglucosamine backbone and is correlated with the host range of the infecting bacterium (Roche et al., 1991). Purified Nod factor triggers a subset of the host responses observed upon inoculation with compatible *Rhizobium*, including root hair deformation, morphogenesis of nodule-like structures, and expression of certain nodule-specific genes or "nodulins" (Lerouge et al., 1990; Truchet et al., 1991; van Brussel et al., 1992; Horvath et al., 1993).

Infection by *Rhizobium* is delayed by one or more days relative to initial inoculation depending on host and bacterial genotypes. This delay constitutes the so-called preinfection stage when rhizobia first encounter the plant root and interact primarily with young emerging root hairs, the site of subsequent infection by the bacterium (Vincent, 1980; Scheres et al., 1990a). In the *R. meliloti–Medicago sativa* (alfalfa) interaction, in which the minimum time to infection is >24 hr (Dudley et al., 1987), the length of the preinfection period varies in relation to quantitative differences in *nod* gene regulation (Kondorosi et al., 1989, 1991), suggesting that signaling may be an important determinant of the preinfection phase. Susceptibility to infection is a transient phenomenon specifically associated with root hair cells that differentiate during the preinfection period (Bhuvaneswari et al., 1981). Because these same cells are also a locus of expression for the early nodulin gene *ENOD12*, Pichon et al. (1992) speculated that expression of early nodulin genes prepares the differentiating root hairs for infection. Despite these indications that events critical to initiation of the symbiosis occur prior to infection, relatively little attention has been given to this phase of the symbiosis; in particular, few plant genes have been identified that are induced prior to infection, and none of them are specific to the preinfection period.

Of known nodulin genes, the most rapidly induced are *ENOD40* and *ENOD12*. The *ENOD40* transcript is first detected in the root pericycle opposite incipient nodule primordia and in the nodule primordium itself (Kouchi and Hata, 1993; Yang

[1] To whom correspondence should be addressed.

et al., 1993; Asad et al., 1994). Expression of *ENOD40* continues throughout nodule development, and in mature soybean nodules, the transcript is localized in the pericycle of vascular bundles and in uninfected cells of the central tissue. For *ENOD12*, early expression occurs in the epidermis of inoculated roots prior to infection by *Rhizobium* (Scheres et al., 1990b; Pichon et al., 1992; Journet et al., 1994). The induction of *ENOD12* prior to infection by *Rhizobium* and its dependence on Nod factor (Scheres et al., 1990b; Journet et al., 1994) provide evidence that both signaling and nodulation-specific gene expression occur several hours in advance of infection. Maximal expression of *ENOD12*, however, is correlated with postinfection events (Scheres et al., 1990a, 1990b; Govers et al., 1991); in particular, during early nodule morphogenesis the *ENOD12* transcript is localized to cells in the vicinity of the growing infection thread and in the nodule primordium, whereas in mature nodules transcript occurs in cells preceding infection (Pichon et al., 1992).

Due to the potential importance of preinfection events in initiation of the symbiosis and the absence of known genes that are specifically and strongly expressed prior to infection, we sought to identify additional early *Rhizobium*-induced genes. We describe here the isolation and characterization of a cDNA clone from the annual legume *M. truncatula* (Barker et al., 1990) that encodes a putative peroxidase protein. We demonstrated that this gene, designated *rip1* for *Rhizobium*-induced peroxidase, is rapidly and transiently induced by compatible *R. meliloti*, that *R. meliloti* Nod factor is both necessary and sufficient for induction, and that the duration of maximal expression coincides with the preinfection period, declining near the onset of infection and nodule morphogenesis. We also demonstrated that although expression precedes bacterial infection, the transcript is localized to differentiating epidermal cells in the root zone that is subsequently infected by *Rhizobium.*

RESULTS

Cloning and Characterization of the *rip1* Peroxidase Gene

To isolate genes induced during early nodule development, we used a polymerase chain reaction (PCR)–based subtractive hybridization method that enriches conditionally expressed genes (Wang and Brown, 1991). Starting material consisted of cDNA prepared from control root mRNA (uninoculated) and mRNA isolated from roots 48 or 108 hr after inoculation with *R. meliloti.* The enrichment process consisted of repeated rounds of subtraction and PCR amplification, resulting in the suppression of common "root" cDNAs and the indirect enrichment of nodule-specific cDNAs.

To evaluate the success of the subtractive enrichment, we prepared blots containing unenriched cDNA from control and *Rhizobium*-inoculated roots and enriched cDNA obtained from the same control and inoculated roots after three rounds of subtractive hybridization and PCR amplification. For probes, we used the soybean actin gene (Shah et al., 1982) as a common root gene control and the *M. truncatula* gene *ENOD11* (D. Barker, unpublished data) as an early nodulin gene control. Figure 1 shows that prior to subtraction, the actin transcript was readily detected in all unenriched samples, consistent with its identity as a "common root gene." After subtraction, however, the actin transcript was no longer detected (Figure 1); thus, common root genes were suppressed by subtraction. When *ENOD11* was used as probe, the transcript was detected only in cDNA from inoculated roots, consistent with its identity as an early nodulin gene. Following three rounds of subtraction and PCR amplification, the *ENOD11* transcript was substantially enriched in these same inoculated root samples (Figure 1). A similar result was obtained for the early nodulin gene *ENOD12* (data not shown). Based on the apparent success of the subtractive hybridization, we screened a plasmid library constructed from the enriched cDNA fractions. Single clones were chosen at random to probe blots containing cDNA from inoculated and control roots. One clone, named G2A11, hybridized with the unenriched 48-hr sample but not with the unenriched 0- or 108-hr samples (Figure 1). Thus, G2A11 appeared to represent a gene that was transiently induced during early nodule development.

Sequencing of the 264-bp cDNA fragment of G2A11 revealed a single open reading frame spanning the entire length of the clone. We postulated that G2A11 is the fragment of a larger cDNA; this result could be expected based on the RsaI/AluI enzyme digestion of the cDNA starting material (see Methods). Comparison with sequences at the National Center for Biotechnology Information revealed that a potential amino acid sequence encoded by G2A11 shares high homology with more than 30 plant peroxidase proteins. The highest homologies, without considering conservative amino acid substitutions, were with legume peroxidase genes expressed in cell cultures of peanut (57%; Buffard et al., 1990) and lupine (53%; Perrey et al., 1991) and pathogenesis-related peroxidase genes from wheat (52%; Rebmann et al., 1991), barley (51%; Thordal-Christensen et al., 1992), and rice (52%; Reimmann et al., 1992). Each of these peroxidase genes encodes a transcript of ~1.3 kb, in good agreement with size estimates for the G2A11-related transcript.

To estimate the copy number of the *rip1* gene in *M. truncatula*, DNA gel blots of genomic DNA from ecotypes A-68 and A-17 were probed with the *rip1* cDNA clone G2A11. Results from the analysis of four separate restriction enzyme digests, including EcoRI, EcoRV, BamHI, and ScaI, none of which cuts within the G2A11 cDNA sequence, are given in Figure 2. When hybridized with A-68, only a single fragment was obtained in DNA digested with EcoRI, EcoRV, or ScaI (Figure 2B, lanes 1, 2, and 4), consistent with the existence of a single copy of *rip1* in *M. truncatula* A-68. However, when DNA was digested with BamHI, two hybridizing fragments were obtained (Figure 2B, lane 2), suggesting the existence of a second gene or perhaps the existence of a BamHI site within the G2A11 genomic sequence. A similar overall pattern of hybridization

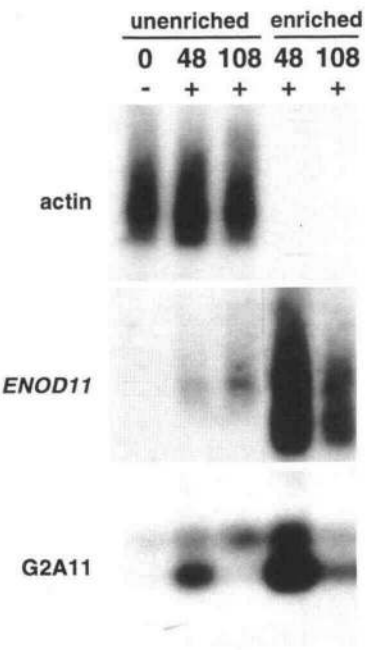

Figure 1. Characterization of the Subtractive Library.

Autoradiographs of identical 1% agarose gel blots probed with ^{32}P-labeled actin, *ENOD11*, or G2A11, as indicated, are shown. Each blot contains cDNA from uninoculated roots (labeled 0) and cDNA from *Rhizobium*-induced roots 48 or 108 hr after inoculation (labeled 48+ or 108+, respectively). Unenriched samples correspond to the original, nonsubtracted cDNA population. Enriched samples were the product of three rounds of subtractive hybridization and PCR amplification.

was obtained with genotype A-17, with the exception that digestion with EcoRV or ScaI each revealed an additional fragment (Figure 2A, lanes 2 and 4, respectively) and digestion with EcoRI revealed three additional hybridizing fragments (Figure 2A, lane 1). To determine whether the multiple EcoRI fragments were the result of heterozygosity at the *rip1* locus or perhaps allelic diversity within the A-17 population, we analyzed DNA from 10 sibling plants. All 10 siblings gave the original four-band hybridization pattern in EcoRI-digested DNA, indicating the existence of multiple, probably homozygous, loci with homology to G2A11 (data not shown).

Using the G2A11 cDNA as probe, we isolated three apparently overlapping clones from a genomic library of *M. truncatula* cv Jemalong, each of which contained a 2.3-kb EcoRI fragment that hybridized to G2A11 (data not shown). Figure 3 shows the DNA sequence derived from one of these clones. Analysis of potential translation products revealed three consecutive open reading frames (putative exons) that have high homology with known plant peroxidase genes and that are bordered by sequences homologous to the consensus 5′ and 3′ splice sites of plants (compiled by Brown, 1986). The predicted translation start site has a context similar to the consensus for translation initiation in plants (Lütcke et al., 1987) and would result in a preprotein of similar size to that predicted for other plant peroxidases. A 264-nucleotide stretch in the third exon is 98% identical to the entire G2A11 cDNA sequence (Figure 3, underlined). At present, we are unable to determine whether (1) G2A11 is the product of a gene different from that given in Figure 3 or (2) the 2% sequence divergence is an artifact of the multiple rounds of PCR used to enrich G2A11. The fact that all four nucleotide changes are associated with first and second codon positions, and not the typically more variable third position, supports the latter possibility.

As shown in Figure 4, the predicted amino acid sequence is closely related to that of several other plant peroxidases, including those derived from cDNAs of peanut (Pnc1; Buffard et al., 1990), rice (Pir3; Reimmann et al., 1992), and tobacco (TOBANPER; Criqui et al., 1992), and the protein sequence of TP7 from turnip (Mazza and Welinder, 1980). The N-terminal 27 amino acids constitute a putative membrane translocation signal sequence, with a hydrophobic core and predicted cleavage site at alanine 27 that conform closely to the rules of von Heijne (1983). Distal to the putative signal peptide, the highest level of identity (59%) is with Pnc1 from peanut. Several of the sequence motifs given in the Figure 4 consensus sequence are widely conserved among plant peroxidases (Tyson, 1991, 1992), including the context of the distal and proximal heme

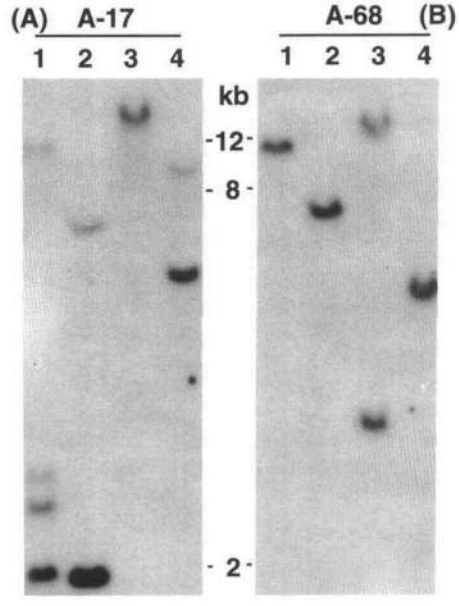

Figure 2. Gel Blots of DNA from *M. truncatula* Ecotypes A-17 and A-68 Probed with the *rip1* cDNA Clone G2A11.

Each lane contains 5 μg of restriction enzyme–digested DNA resolved on a 0.6% agarose gel. The 12, 8, and 2 kb indicate the position of migration for size marker standards.

(A) DNA from ecotype A-17 digested with EcoRI (lane 1), EcoRV (lane 2), BamHI (lane 3), and ScaI (lane 4).

(B) DNA from ecotype A-68 digested with EcoRI (lane 1), EcoRV (lane 2), BamHI (lane 3), and ScaI (lane 4).

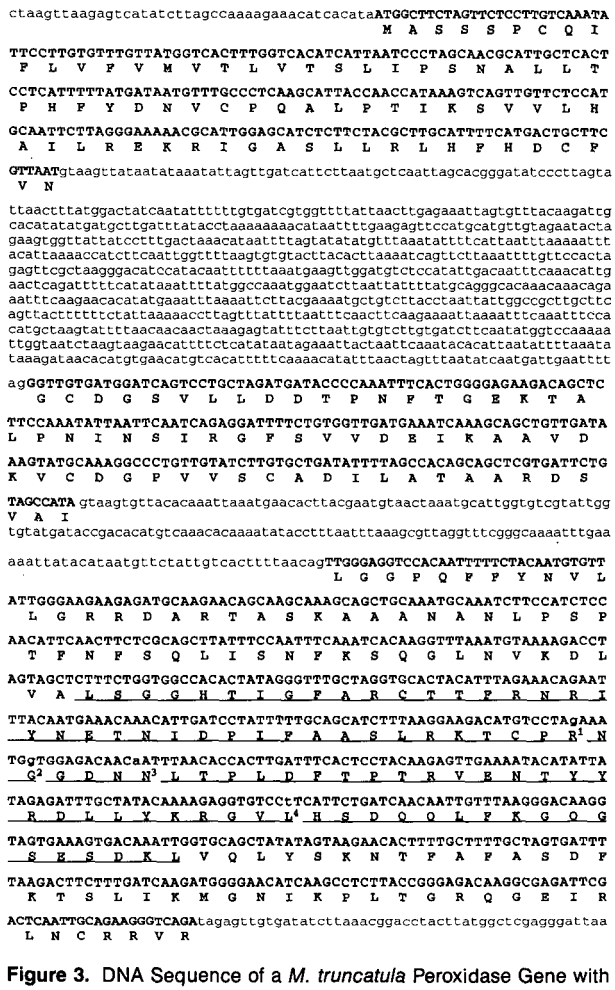

Figure 3. DNA Sequence of a *M. truncatula* Peroxidase Gene with Homology to the G2A11 cDNA Clone.

The nucleotide sequences of open reading frames with homology to known peroxidase genes are indicated by boldface uppercase letters. Predicted 5′ and 3′ untranslated regions and putative intron sequences are indicated by lowercase letters. Sequence homology with G2A11 cDNA is underlined. The predicted amino acid sequence is given in uppercase letters beneath the nucleotide sequence. Points of difference between the nucleotide sequence shown and that of G2A11 are indicated by superscripts and lowercase letters. The corresponding G2A11 nucleotides are A, A, G, and A (superscripts 1, 2, 3, and 4, respectively).

group ligands at histidines 67 (R·GASL·RLHFHDCFV·GCD·S·LLD) and 199 (VALSGAHT·G); cysteine residues at positions 38, 71, 76, 118, 125, 232, and 325; and potential glycosylation sites at asparagines 97, 165, 216, and 256.

Time Course of *rip1* Induction by *R. meliloti*

To confirm the earlier observation that *rip1* was induced transiently upon inoculation with *R. meliloti* (Figure 1) and to allow

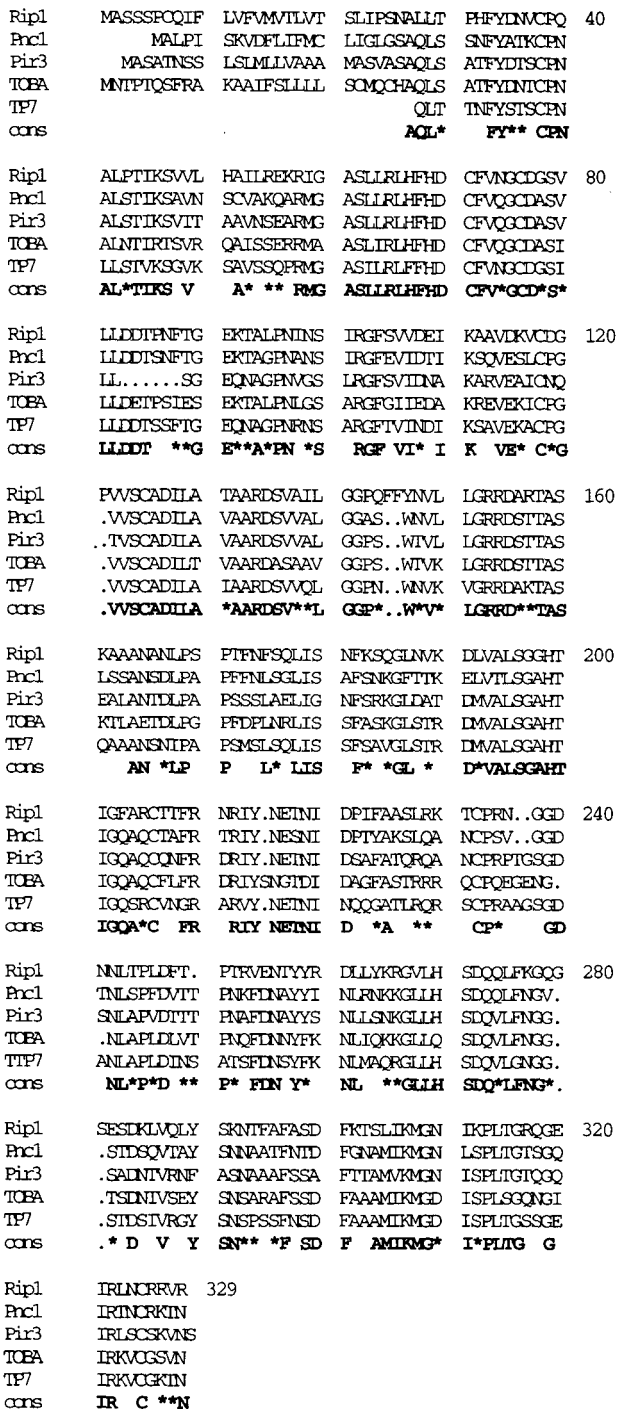

Figure 4. Alignment of the Derived *M. truncatula* Peroxidase Protein Sequence with That of Pnc1, Pir3, TOBANPER, and TP7.

Identities are shown in the consensus sequence (labeled cons) where four or more identical amino acids are considered a consensus. Asterisks indicate the occurrence of three identical amino acid residues. Dots indicate gaps in the amino acid sequence used to align the sequences. TOBA, TOBANPER.

comparison of transcript levels throughout nodule development, total RNA was isolated from the roots and shoots of inoculated plants beginning at 6 hr postinoculation (preinfection) and through 16 days (nodule function). In addition, we followed the time course of nodule development by microscopy to compare changes in *rip1* transcript with early infection events. As shown in Figure 5, uninoculated roots (0 hr) consistently exhibited a low level of hybridization with the *rip1* probe, whereas hybridization was never detected with shoot RNA from either inoculated or uninoculated plants, indicating that basal expression of *rip1* is specific to roots. After inoculation with *R. meliloti*, there was a rapid increase in *rip1* message, with maximum levels already present by the 6-hr time point. This high level of transcript was maintained throughout the preinfection period (6 through 24 hr; Figure 5) and declined coincident with the onset of infection and the appearance of microscopic nodule primordia at ~48 hr. Throughout early nodule morphogenesis (48 to 96 hr), the *rip1* message remained at this lower induced level and subsequently declined to a level below that first observed in uninoculated roots. To define the initial induction of *rip1* more completely, we analyzed samples of total root RNA collected between 0 and 6 hr postinoculation. The data presented in Figure 6 show that elevated levels of transcript were near maximal by 3 hr postinoculation, well in advance of root hair deformation and bacterial infection that are most prominent near 48 hr. A control hybridization with the soybean actin gene demonstrated that RNA concentrations in each lane were approximately equal.

As a positive control for nodule-specific gene expression, RNA gel blots were probed with a second cDNA clone, designated p54, that we also isolated from the subtractive library. Based on DNA sequence comparisons, p54 is the 3′ cDNA fragment of the early nodulin gene *ENOD11*, which was identified by D. Barker (unpublished data). *ENOD11* encodes a putative repetitive proline-rich protein similar to that encoded by *ENOD12*, with similar patterns of symbiotic expression. From microscopic examination of inoculated roots, we determined that changes in the abundance of *ENOD11* transcript provided an excellent marker for early nodulation events. The *ENOD11* transcript was first detected near 48 hr, coincident with infection initiation and the development of microscopic nodule primordia. Transcript levels were maximal at 72 hr, when macroscopic nodule primordia were first evident, and were maintained at a lower induced level in mature nodules (Figure 5).

Nod Factor Is Necessary and Sufficient for Induction of *rip1*

Rhizobium Nod factor is required both for nodule morphogenesis and for the induction of several early nodulin genes. To determine whether Nod factor was also involved in *rip1* induction, we analyzed *rip1* transcript after inoculation of roots with wild-type *R. meliloti* 1021 or its Nod factor–deficient derivatives, SL44 and TJA1A3T. Strain SL44 contains a deletion of the *nodD1–nodABC* region, which should affect Nod factor biosynthesis and expression of *nodD1*-dependent genes, whereas strain TJA1A3T contains a Tn*5* insertion in *nodA* in which the primary defect should be an inability to synthesize the *N*-acetylglucosamine backbone of Nod factor.

As shown in Figure 7, *rip1* was rapidly and transiently induced by wild-type *R. meliloti* 1021, consistent with results obtained previously with strain ABS7 (shown in Figure 5). Elevated levels of transcript, evident by the first time point at

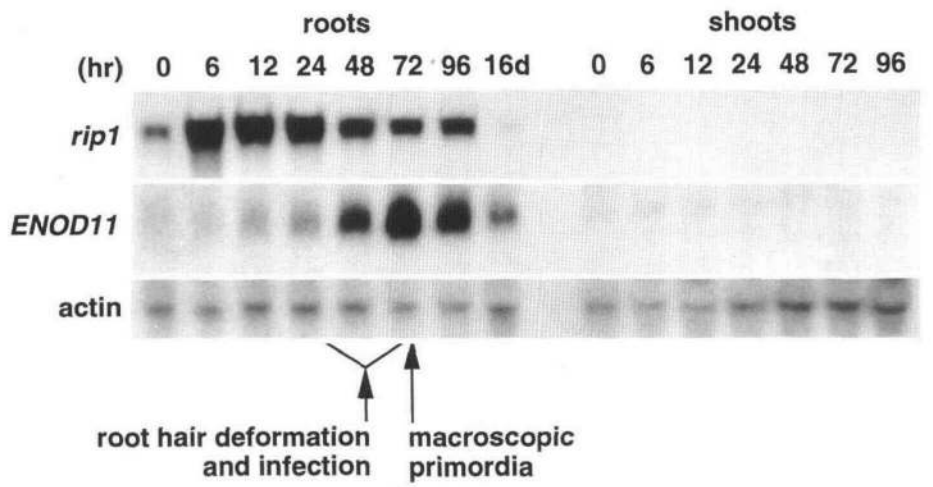

Figure 5. Induction of *rip1* and *ENOD11* Transcripts by *R. meliloti* ABS7.

Autoradiographs of replicate gel blots containing total RNA isolated from the roots and shoots of plants after inoculation with *R. meliloti* ABS7 are shown. Each lane contains RNA equivalent to 0.2 g fresh weight of tissue. Blots were probed with ^{32}P-labeled G2A11 (*rip1*), p54 (*ENOD11*), or actin, as indicated. Arrows indicate the initial incidence of infection and root hair deformation and of macroscopic nodule primordia. Time is reported in hours, with the exception of the 16-day time point, which is indicated as 16d.

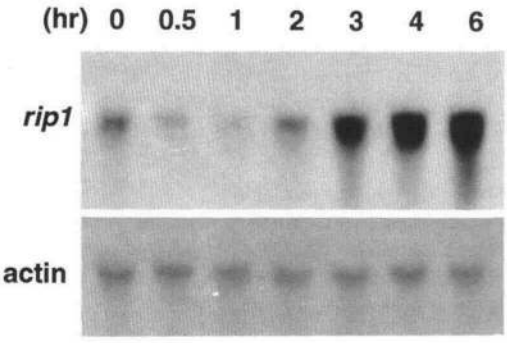

Figure 6. Early Time Course of *rip1* Induction.

Gel blots of total root RNA isolated from roots at various times between 0 and 6 hr after inoculation with *R. meliloti* ABS7 are shown. Each lane contains RNA equivalent to 0.2 g fresh weight of root tissue. A single RNA gel blot was first probed with G2A11 (*rip1*) and then stripped and reprobed with actin, as indicated. No signal could be detected when hybridized with ^{32}P-labeled p54 (*ENOD11*) or *ENOD12* probes (data not shown).

12 hr, were maintained through 48 hr, and the subsequent decline by 100 hr correlated with the appearance of macroscopic nodule primordia. Interestingly, maximal induction of *rip1* by *R. meliloti* 1021 was prolonged relative to that observed with *R. meliloti* ABS7 (compare Figure 7 with Figure 5). This difference was correlated with the timing of appearance of macroscopic primordia for the two strains: *R. meliloti* 1021 consistently gave a delayed induction of macroscopic nodule primordia (by ~24 hr) when compared with *R. meliloti* ABS7.

In experiments with the *R. meliloti* 1021 *nod* gene mutants SL44 and TJA1A3T, neither strain was able to induce the *rip1* transcript (Figure 7 and data not shown). Similarly, neither strain was able to induce the formation of macroscopic nodule primordia, which is consistent with their nodulation-minus phenotype. For comparative purposes, replicate RNA gel blots were probed with *ENOD12* (shown previously to require bacterial *nod* genes for induction; Scheres et al., 1990b) and *ENOD11*. Both genes were induced by wild-type *R. meliloti* 1021 but not by SL44 or TJA1A3T (Figure 7 and data not shown). In agreement with our previous results for strain ABS7 (shown in Figure 5), maximal induction of *ENOD11* by *R. meliloti* 1021 correlated with the appearance of macroscopic nodule primordia. A similar pattern of expression was obtained for *ENOD12*, except that the occurrence of maximal levels of the transcript was slightly delayed (Figure 7).

The preceding results were consistent with a requirement for Nod factor in *rip1* induction, and they eliminated the trivial possibility that *rip1* induction was an artifact of bacterial inoculation. To determine whether Nod factor was sufficient for *rip1* induction, root systems were treated with 5×10^{-9} M purified Nod factor (NodRm-IV[Ac, S] and NodRm-IV[S], [3:1]), and RNA was isolated at various times for gel blot analysis. As shown in Figure 8, elevated levels of the *rip1* transcript were evident within 6 hr after Nod factor treatment and remained high through the final 72-hr time point. In contrast, when replicate blots were probed with *ENOD11* or *ENOD12*, the corresponding transcripts could not be detected even following prolonged exposure (data not shown).

Spatial Distribution of *rip1* Expression Relative to Subsequent Nodule Development

We used a modified tissue printing method (termed "squash blot") to localize the *rip1* transcript in whole root systems and to determine its spatial relationship to the zone of subsequent nodule emergence. Prior to inoculation with *R. meliloti*, the *rip1* transcript could not be detected on squash blots (data not shown), which is consistent with the low level of basal expression detected in RNA gel blots. As shown in Figure 9A, by 14 hr postinoculation, when *rip1* expression should be maximal, the transcript was detected in tissue adjacent to the root tip. To verify the results obtained by squash blot analysis, we dissected roots at 12 hr postinoculation and analyzed the corresponding RNA by gel blot analysis. The data in Figure 9B show that the *rip1* message was confined primarily to the root tip. Based on densitometry analysis of autoradiographs, we estimated that the concentration of *rip1* message was at least 40-fold greater within 1 cm of the root tip than in the remaining portion of the root. To examine the physical correlation between the distribution of the *rip1* transcript at 12 hr postinoculation (Figure 9) and the zone of subsequent nodule development, we marked

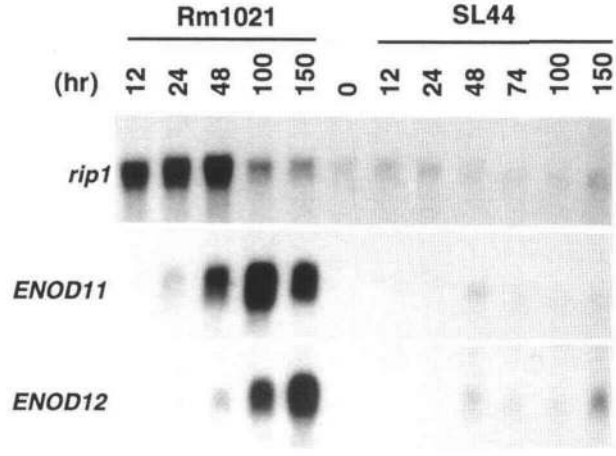

Figure 7. Induction of *rip1*, *ENOD11*, and *ENOD12* by *R. meliloti* 1021 and Its Nodulation-Deficient Derivative SL44.

Autoradiographs of replicate gel blots containing total RNA isolated from the roots of plants after inoculation with *R. meliloti* 1021 (Rm 1021) or *R. meliloti* SL44 are shown. Each lane contains RNA equivalent to 0.2 g fresh weight of tissue. Blots were probed with ^{32}P-labeled G2A11 (*rip1*), p54 (*ENOD11*), or *ENOD12*, as indicated. Time is reported in hours.

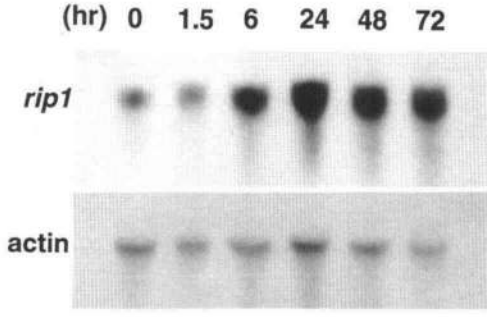

Figure 8. Induction of *rip1* by 5 × 10^{-9} M Nod Factor.

Gel blots of total root RNA after application of the primary *R. meliloti* 1021 Nod factors NodRm-IV(Ac, S) and NodRm-IV(S), (3:1) are shown. Each lane contains RNA equivalent to 0.2 g fresh weight of tissue. Blots were probed with ^{32}P-labeled G2A11 (*rip1*) or actin, as indicated. Time is reported in hours.

main root tips by spot treatment with methylene blue and followed nodule morphogenesis by microscopy. We determined that nodule primordia, which are readily visible at 72 hr, form primarily within a narrow zone (≤2 cm in length) near the position of the root tip at the time of initial encounter with *Rhizobium* (data not shown). Furthermore, nodulation was observed only on the main and large lateral roots, which is consistent with the distribution of the *rip1* transcript revealed by squash blot analysis. Taken together, these data indicate that the distribution of developing nodules at 72 hr corresponds to the root zone where the *rip1* transcript was detected at 14 hr postinoculation.

For precise localization of the *rip1* transcript, we used in situ hybridization to examine paraffin sections of root tissue from inoculated and uninoculated plants. Although the analysis focused primarily on tissue from within 2 cm of the root tip, to provide continuity with data from squash blots and root dissections (Figure 9), we also analyzed tissue selected at random from mature portions of the root and from lateral root branch points. As shown in Figures 10A and 10B, uninoculated plants exhibited a low level of hybridization in developing vascular tissue. After inoculation with *R. meliloti*, there was a marked increase in hybridization to the vascular cylinder and the appearance of strong hybridization in the root epidermis, including differentiating root hairs (Figures 10C and 10D). From analysis of consecutive serial sections, the *rip1* transcript appeared to be uniformly induced throughout most, if not all, of the differentiating epidermal cells, extending from the root meristem through the zone of root hair differentiation. Similar analyses with the sense probe gave negligible signal on sections of developing root tips 12 hr after inoculation (Figures 10E and 10F), indicating that hybridization was specific to the coding strand of *rip1*. The transcript was not detected in sections taken from mature portions of the root or from lateral root branch points (data not shown), confirming our earlier observation that the transcript was concentrated in the root tip (Figure 9).

DISCUSSION

Recently, substantial progress has been made toward understanding the role of bacterial genes and gene products in nodule initiation and development. By comparison, however, relatively little progress has been made toward understanding the role of plant genes in the interaction, particularly during preinfection, when primary determinative events of the symbiosis are likely to occur (see Introduction). In this study, we

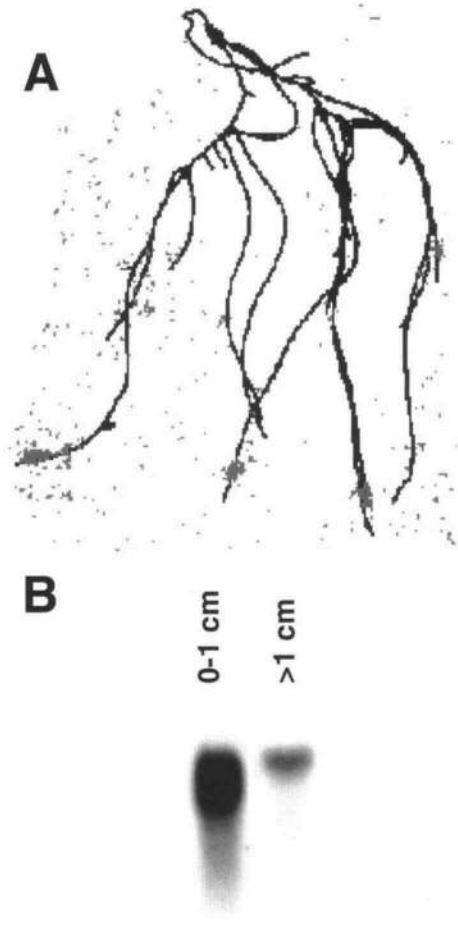

Figure 9. Spatial Distribution of the *rip1* Transcript in Whole Root Systems of *M. truncatula*.

(A) Squash blot of a whole root system 14 hr after inoculation with *R. meliloti* ABS7. Red coloration corresponds to hybridization signal detected with a Betagen Betascope blot analyzer.

(B) RNA gel blots of whole root dissections 12 hr after inoculation with *R. meliloti* ABS7 probed with ^{32}P-labeled G2A11 (*rip1*). Lanes contain total RNA isolated from the first 1-cm interval adjacent to the main root tip (0 to 1 cm) or from the remaining portion of the main root (>1 cm), as indicated. Based on fresh weight measurements, there is a minimum 15-fold excess of total RNA in the >1 cm lane.

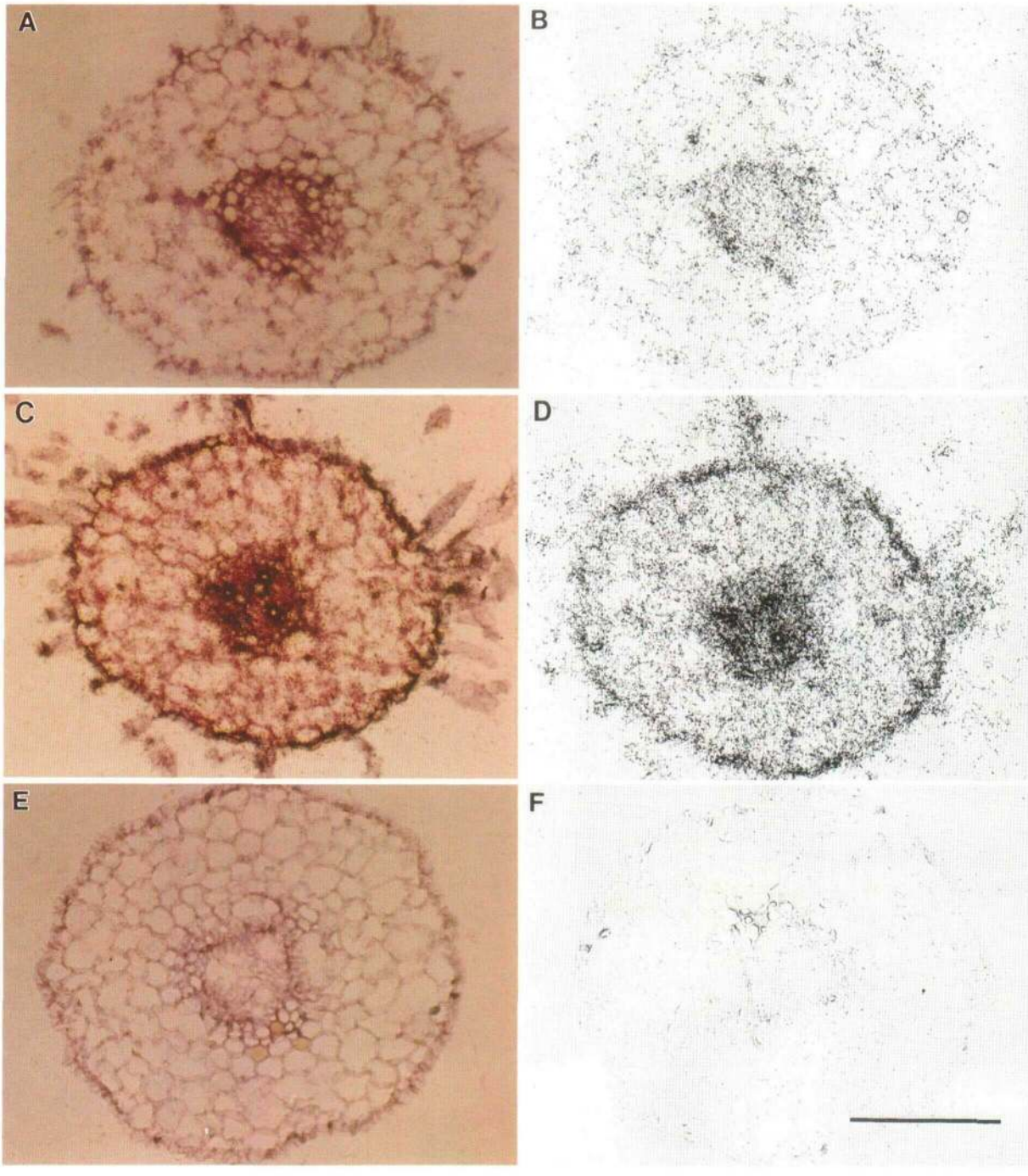

Figure 10. In Situ Hybridization of *M. truncatula* Root Sections Collected Immediately before and 12 Hr after Inoculation with *R. meliloti* ABS7.

Bright-field micrographs of 10-μm tissue sections taken from the terminal 1 cm of main roots and hybridized with ^{35}S-labeled G2A11 (*rip1*) riboprobe are shown. **(A)**, **(C)**, and **(E)** were stained with azure II and methylene blue. Adjacent panels (**[A]** and **[B]**, or **[C]** and **[D]**, or **[E]** and **[F]**) are the same specimen after and before staining, respectively.

(A) and **(B)** Section from an uninoculated root hybridized with antisense *rip1* probe.

(C) and **(D)** Section from a root 12 hr after inoculation with *R. meliloti* ABS7 hybridized with antisense *rip1* riboprobe. Silver grains appear as dark spots. Note the intense signal present in the epidermis, including root hairs, and in the vasculature, particularly as compared with similar sections from uninoculated roots (**[A]** and **[B]**).

(E) and **(F)** Section from an inoculated root hybridized with sense *rip1* probe.

Bar = 0.5 mm.

employed a subtractive hybridization–PCR method to isolate genes induced by *R. meliloti* in the annual legume *M. truncatula.* One of these genes, designated *rip1*, shares high homology with the predicted amino acid sequence of numerous plant peroxidase genes. *rip1* is distinct from other early nodulin genes not only in its putative enzyme product but also in its strong, transient induction prior to rhizobial infection. The transcript for *rip1* was nearly maximal by 3 hr postinoculation, remained high throughout the preinfection period, and declined by 48 hr at the onset of infection and nodule morphogenesis. By contrast, maximal induction of other early nodulin genes is associated with rhizobial infection and early nodule morphogenesis, and these genes continue to be expressed in mature nodules. Thus, *rip1* represents a new class of *Rhizobium*-induced genes whose peak expression is correlated with the preinfection period.

An intriguing aspect of *rip1* regulation is that although its induction preceded infection and formation of nodule primordia by nearly 48 hr, the transcript was localized within differentiating epidermal cells in the root zone subsequently infected by *Rhizobium.* Bhuvaneswari et al. (1981) observed that infection of alfalfa by *R. meliloti* occurs predominantly in root hair cells that differentiate during the preinfection period; we have observed a similar situation with *M. truncatula.* Thus, susceptibility to rhizobial infection, which is a transient phenomenon, was correlated both spatially and temporally with the induction of *rip1* expression. Epidermal cells within the susceptible root zone are also the site of early *ENOD12* (Pichon et al., 1992; Journet et al., 1994) expression, as seen by promoter–β-glucuronidase gene fusions in transgenic plants, indicating that multiple symbiosis-related genes are induced in the cell type destined for infection. However, although the spatial distribution of *ENOD12* expression during preinfection appears similar if not identical to that of *rip1*, the preinfection level of *ENOD12* transcript is low and can be detected only by sensitive means such as reverse transcriptase–PCR (Scheres et al., 1990b); high levels of the *ENOD12* transcript are correlated instead with infection and nodule morphogenesis. Thus, the strong, rapid induction of *rip1* prior to rhizobial infection and its subsequent decline at the onset of infection and morphogenesis distinguish it from *ENOD12* and indicate that *rip1* is regulated by a different mechanism. This difference is further underscored by the observation that whereas Nod factor was both necessary and sufficient for induction of *rip1*, it was required but not sufficient for induction of detectable levels of *ENOD11* or *ENOD12* when assayed on gel blots of total RNA. In previous reports of *ENOD12* induction by Nod factor in pea (Scheres et al., 1990b; Horvath et al., 1993) and alfalfa (Journet et al., 1994), detection relied on more sensitive, but semiquantitative methods (reverse transcriptase–PCR and β-glucuronidase reporter gene expression, respectively). Thus, Nod factor is sufficient to reproduce, quantitatively, the preinfection phenotype of both *rip1* and *ENOD12* but not the main increase in the *ENOD12* transcript associated with rhizobial infection and early nodule morphogenesis. The low-level induction of *ENOD12* by Nod factor may be a consequence of the inefficient induction of nodule primordia, a primary locus of *ENOD12* expression. Despite these apparent differences in the regulation of early nodulin genes, the existence of a *Rhizobium*-inducible transcriptional mechanism(s) that is activated prior to infection in the differentiating epidermis is consistent with the model proposed by Bhuvaneswari et al. (1981; see also Pichon et al., 1992), wherein a class of *Rhizobium*-susceptible root hair cells differentiate during the preinfection period.

Several early nodulin genes, including *ENOD12* (Scheres et al., 1990b; Pichon et al., 1992), *ENOD10* (Lobler and Hirsch, 1993), *MtPRP4* (Wilson et al., 1994), and *ENOD11* (D. Barker, unpublished data), encode putative repetitive proline-rich proteins (PRPs) that are members of the extensin superfamily of cell wall proteins (Kieliszewski and Lamport, 1994). These nodule-specific PRPs contain a conserved N-terminal signal sequence typical of cell wall proteins and, with the exception of *ENOD12*, all contain the pentapeptide motif PPXYK, which has been implicated in covalent intermolecular cross-linking of certain PRPs (Bradley et al., 1992; Kieliszewski and Lamport, 1994). Cross-linking of cell wall proteins is presumed to be mediated by cell wall–bound peroxidases and requires production of substrate hydrogen peroxide. Thus, the physical coincidence of the Rip1 protein and substrate PRPs might provide a mechanism for cell wall modification that could be activated at specific sites by production of hydrogen peroxide. It will be necessary, however, to localize the *Rhizobium*-induced peroxidase protein, substrate PRPs, and the presumed oxidative burst (Apostol et al., 1989) before this hypothesis can be critically tested.

Cross-linking of cell wall–associated proteins provides a potential mechanism for altering cell wall architecture during plant growth and development (Cordewener et al., 1991; van Engelen and de Vries, 1992; Zheng and van Huystee, 1992). It is possible, therefore, that the *rip1* peroxidase may act to facilitate infection, perhaps by contributing to repair of the cell wall at the site of infection, as suggested by Salzwedel and Dazzo (1993), or to the formation of novel cell wall structures (e.g., those associated with susceptible root hairs). For example, PRPs are abundant within the infection thread matrix (Sherrier and VandenBosch, 1994), as is a high molecular weight glycoprotein (VandenBosch et al., 1989) that has been shown to become oxidatively cross-linked by the same mechanism (Bradley et al., 1992). In plant–pathogen interactions, in which peroxidase and structural wall protein genes are frequently coinduced, cell wall cross-linking may provide a mechanism for limiting pathogen ingress (Bradley et al., 1992). Thus, it is equally possible that *rip1* peroxidase activity functions to restrict rhizobial infection in a manner analogous to mechanisms that occur in plant–pathogen interactions. In this regard, it is well established that even in compatible *Rhizobium*–legume interactions, many infections terminate after the infection thread penetrates only one or a few cells (Caetano-Anollés and Gresshoff, 1991). Vasse et al. (1993) determined that this

arrest of infection during nodule development shares many features with defense responses to pathogens, such as elevated levels of defense-related proteins (phenylalanine ammonia-lyase, chalcone synthase, acidic chitinase, and hydroxyproline-rich glycoproteins). We have observed apparently similar arrested infections in *M. truncatula*; these infections are distinguished from successful infection events by strong autofluorescence (D. Dreyer and D. Cook, unpublished data). If these events constitute a modified defense response, then peroxidase activity would be strongly implicated in the associated cell wall fortification.

rip1 adds to a growing list of genes whose expression is induced by compatible rhizobia but are also expressed in other plant tissues. For example, in addition to their expression during early nodule development, both *ENOD40* and *ENOD12* are expressed in stem, or stem and flower tissue, respectively (Scheres et al., 1990b; Govers et al., 1991; Yang et al., 1993). The finding that many nodulin genes also exhibit nonsymbiotic expression is not surprising because nodulation probably arose, in part, by diversion of mechanisms for other aspects of plant growth and development, including plant–pathogen interactions. Likely scenarios for recruitment of genes for purposes of nodulation include expanding the regulation of nonsymbiotic genes to include nodule-specific expression, as appears to be the case for *PsENOD12* (Scheres et al., 1990b), or gene duplication with subsequent specialization of one locus for nodule-specific regulation/function. For *rip1*, DNA gel blot data are consistent with gene duplication, although whether one locus has diverged specifically for purposes of nodulation is uncertain. For example, it remains to be determined whether the *rip1* transcript detected in uninoculated roots derives from the same gene as that detected after inoculation with *R. meliloti.*

The spatial and temporal patterns of *rip1* expression suggest that transcription of this gene is likely to be tightly controlled; however, the rapid, transient nature of *rip1* induction indicates that the regulation of *rip1* may be different from that of other early nodulin genes, such as *ENOD12.* In fact, the transient expression pattern of *rip1* is typical of what one might expect of genes down-regulated by feedback inhibition of nodulation (Bhuvaneswari et al., 1981; Caetano-Anollés and Gresshoff, 1991). Consistent with this model, recent results from our laboratory (D. Dreyer, unpublished data) indicate that the reduced level of the *rip1* transcript that is temporally correlated with early nodule morphogenesis is physically associated with the previously established infection zone and not the newly differentiating root hair zone. Finally, it is intriguing that the *rip1* transcript is declining at a time when transcripts of other nodulin genes, such as *ENOD12* (Scheres et al., 1990a, 1990b) and *ENOD11*, are increasing. Resolution of this apparent contradiction may require a less simplistic view of the regulation of early nodulin genes. Thus, we anticipate that *rip1* will provide a valuable tool to examine regulation of gene expression during early nodulation as well as to examine probable changes in cell wall architecture associated with early symbiotic interactions.

METHODS

Plant Material and Growth Conditions

Medicago truncatula genotypes A-17 and A-68 represent selections from different ecotypes. For nodulation experiments, plants of A-17 were grown aeroponically and inoculated with *Rhizobium meliloti* essentially as described by Gallusci et al. (1991). Briefly, plants were grown in inorganic nutrient media (Lullien et al., 1987) containing 5 mM NH_4NO_3 for 2 weeks, at which time they were transferred to fresh media lacking NH_4NO_3 and grown for an additional 4 days before inoculation with *R. meliloti* or treatment with Nod factors. For inoculation, bacteria were grown to late log phase in broth cultures, washed by centrifugation, and added directly to nutrient media in the aeroponic chambers. Under these conditions, nodulation was rapid and uniform. All nodulation experiments were conducted with a 12-hr photoperiod (18°C night/22°C day) with a light intensity of 300 μmol m^{-2} sec^{-1}. For Nod factor treatment, purified Nod factor was resuspended in 200 μL of water and added directly to nutrient media in the aeroponic chambers to give a final concentration of 5×10^{-9} M.

Nucleic Acid Isolation and Gel Blot Analysis

DNA was isolated from fresh or frozen tissue by extraction with hexadecyltrimethylammonium bromide according to the method of Rogers and Bendich (1988). For large-scale isolations, DNA was purified further by CsCl density gradient centrifugation. For RNA isolation, tissue samples were quick frozen in liquid nitrogen and either extracted immediately or stored at −80°C. Frozen tissue was ground to a powder by mortar and pestle in liquid nitrogen, resuspended in CSB buffer (7.5 M guanidine HCl, 25 mM sodium citrate, 0.5% sodium lauryl sarcosine, 0.1 M β-mercaptoethanol), and homogenized in a polytron for 30 sec. The homogenate was mixed with 2 M sodium acetate, pH 4.0, extracted with an equal volume of phenol–chloroform (1:1), and centrifuged until the phases were separated and the particulate interface was firm. The upper, aqueous phase was collected and precipitated with an equal volume of isopropanol at −20°C. RNA was recovered by centrifugation, resuspended in CSB, and precipitated again with isopropanol. The purified RNA pellet was resuspended in RNase-free water and either used directly or stored at −80°C after mixing with 3 volumes of absolute ethanol and one-tenth volume of 3 M sodium acetate, pH 5.2. General nucleic acid manipulations, including DNA gel electrophoresis, RNA formaldehyde gel electrophoresis, and transfer of nucleic acids to nylon membranes, were as described by Sambrook et al. (1989). Radioactive probes were prepared by incorporation of α-^{32}P-dCTP using the oligolabeling procedure of Feinberg and Vogelstein (1983). Hybridization was conducted at 60°C in a solution of 7% SDS, 0.25 M NaH_2PO_4, pH 7.0, 0.1 mM EDTA. After overnight hybridization, filters were washed successively in solutions of 0.1% SDS, 2 × SSC (1 × SSC is 0.15 M NaCl, 0.015 M sodium citrate) (21°C for 15 min); 0.1% SDS, 0.1 × SSC (21°C for 15 min); and 0.1% SDS, 0.1 × SSC (65°C for 1 hr).

Squash Blot Analysis

Whole root systems were arranged between two nylon membranes that were themselves placed between a double thickness of Whatman No. 3MM chromatography paper. Tissue was squashed by rolling

a 1-L reagent bottle over the membrane sandwich with firm, constant pressure. After removal of the squashed root system, membranes were exposed to a UV light source for cross-linking of nucleic acids and washed for 1 hr at 65°C in 0.1 × SSC, 0.5% SDS. Hybridization and washing were as previously described. Hybridized probe was detected by conventional autoradiography, which required exposure times of >1 week, or by overnight analysis using a Betagen Betascope 603 blot analyzer.

Subtractive Enrichment

Subtractive hybridization and polymerase chain reaction (PCR) amplification were conducted essentially as described by Wang and Brown (1991). Seedlings of *M. truncatula* A-17 were grown in growth pouches on nitrogen-free Farhaeus medium (Vincent, 1970), and 8-day-old plants were inoculated with *R. meliloti* ABS7. Control plants were maintained under similar conditions but were not inoculated. Roots were harvested either 48 or 108 hr after inoculation, corresponding to early infection and early nodule morphogenesis, respectively. Total RNA was isolated from roots as previously described, and cDNA was prepared using the Fast-trak system (Invitrogen Co., San Diego, CA). To reduce bias due to fragment size during PCR, cDNAs were digested with either AluI or AluI and RsaI, yielding blunt-ended molecules primarily <1 kb in length. Different restriction enzyme digests of the same cDNA samples were pooled and ligated with excess double-stranded oligonucleotide linkers containing one blunt end and one staggered end (5′-TAGTCCGAATTCAAGCAAGAGCACA-3′; 3′-ATCAGGCTTAAGTTCGTTCTC-5′). Thus, all cDNA fragments had identical ends, allowing amplification by PCR using a single oligonucleotide primer (3′-ATCAGGCTTAAGTTCGTTCTC-5′). An EcoRI site near the flush end of the linker facilitates cloning and primer removal. For enrichment of up-regulated genes, cDNA from the uninoculated control roots was used as the "driver," and cDNA from the inoculated roots was used as the "tracer." Driver cDNAs were first digested with EcoRI to remove linker DNAs, thereby preventing PCR amplification in subsequent steps, and then biotinylated with photoprobe biotin (Vector Laboratories, Inc., Burlingame, CA). The biotinylated driver cDNA was mixed with tracer cDNA at a ratio of 20:1, denatured by boiling, and incubated at 68°C to allow complementary strands to reanneal. After reannealing, streptavidin was added to complex the biotinylated cDNAs, and the streptavidin–DNA complexes were removed by extraction with phenol–chloroform. Multiple rounds of subtraction were performed to further the enrichment. After each round of subtractive hybridization, the resulting tracer cDNA was amplified by PCR to provide a sufficient quantity of material for the next round of subtraction.

It is expected that after each round of subtraction, the complexity of the tracer cDNA population will change such that the previous driver cDNA will no longer function efficiently. To compensate for this possibility, a reciprocal subtraction was performed in which the nonenriched control root cDNA was tracer and the inoculated root cDNA was driver. This provided a source of continuously evolving driver cDNA. After three rounds of subtractive enrichment, the amplified tracer cDNA was digested with EcoRI and cloned into the pBluescript KS+ vector (Stratagene). An ordered library of transformants was prepared, and single clones were chosen at random to probe colony blots of the library and gel blots containing cDNA from inoculated and uninoculated roots. By this means, we were able to determine the complexity of the library and whether genes for the individual cDNA clones were induced during nodule development.

DNA Sequencing

The DNA sequence of the *M. truncatula* genomic clone was determined by the dideoxy chain termination method (Sanger et al., 1977) adapted for use in PCR. Templates were double-stranded DNA, and reactions were performed according to the manufacturer's directions using a kit purchased from Epicentre Technologies (Madison, WI). Ambiguities in the DNA sequence were resolved by tailing prematurely terminated products with terminal deoxynucleotidyl transferase (as described in literature available from United States Biochemical Corp., Cleveland, OH): briefly, 1 μL of a reaction mixture containing 5 mM of each dNTP, 3 units of terminal deoxynucleotidyl transferase, and 1 × manufacturer's sequencing buffer was added to each completed sequencing reaction and incubated at 37°C for 30 min before addition of stop buffer. The entire sequence was determined in both directions using DNA primers designed from the previous round of sequence data. The DNA sequence was submitted to GenBank as accession number U16727.

In Situ Hybridizations

Root tissue was harvested and processed by cutting into 0.5- to 1-cm lengths and vacuum infiltrated with 2% formaldehyde and 0.5% glutaraldehyde in 100 mM sodium phosphate buffer, pH 7.2. Tissue was dehydrated in successive ethanol and *t*-butanol graded series and embedded in paraffin. Microtome sections (8 to 10 μm thick) were placed on poly-L-lysine–coated slides. Prior to hybridization, paraffin was removed by extraction with xylene, and the tissue was rehydrated in an ethanol series and double distilled H_2O. Riboprobes were prepared by in vitro transcription of the G2A11 cDNA fragment using either T7 (sense transcript) or T3 (antisense transcript) polymerase and α-^{35}S-UTP (1000 to 1500 Ci/mmol) according to manufacturer's instructions (Stratagene). ^{35}S-labeled transcripts were purified by passage over RNase-free Sephadex G-50 push columns and added directly to the hybridization solution (see following information). Hybridization and subsequent processing were based on the protocol of Cox and Goldberg (1988) with minor modifications according to de Billy et al. (1991). Briefly, rehydrated sections were treated successively with HCl, pronase E, and acetic anhydride to reduce background on subsequent hybridization and to improve penetration of the ^{35}S-labeled riboprobe. Sections were prehybridized in 50% formamide hybridization buffer at 42°C followed by overnight hybridization with sense or antisense ^{35}S-labeled riboprobes under similar conditions. To remove nonhybridized riboprobe, sections were treated with RNase A and washed extensively, concluding with three 40-min high-stringency washes (0.2% SSC at 63°C). For detection of hybridized transcript, slides were coated with Kodak NBT-2 emulsion and exposed for 3 to 10 days in the dark before developing. Specimens were observed by bright-field, dark-field, or Nomarski microscopy using a Zeiss (Batavia, IL) Axioskop light microscope. For staining, specimens were treated briefly (30 sec) with 0.05% azur II and 0.05% methylene blue in 1% sodium metaborate.

ACKNOWLEDGMENTS

This research was supported by United States Department of Agriculture Grant No. 93-37305-9230. We thank David Barker for providing the *ENOD11* and *ENOD12* DNA probes, the *M. truncatula* genomic library, and for helpful comments on the manuscript; Thierry Huguet

for providing *R. meliloti* ABS7 and seed of *M. truncatula* genotypes A-17 and A-68; and Sharon Long, David Ehrhdart, and Morey Atkinson for providing *R. meliloti* strains (*R. meliloti* 1021, SL44, and TJA1A3T) and purified Nod factor.

Received July 1, 1994; accepted November 8, 1994.

REFERENCES

Apostol, I., Heinstein, P.F., and Low, P.S. (1989). Rapid stimulation of an oxidative burst during elicitation of cultured plant cells. Plant Physiol. **90,** 109–116.

Asad, S., Fang, Y., Wycoff, K., and Hirsch, A.M. (1994). Isolation and characterization of cDNA and genomic clones of MsENOD40: Transcripts are detected in meristematic cells. Protoplasma, in press.

Barker, D.G., Bianchi, S., Blondon, F., Dattee, Y., Duc, G., Essad, S., Flament, T., Gallusci, T., Genier, G., Guy, P., Muel, X., Tourner, J., Dénarié, J., and Huguet, T. (1990). *Medicago truncatula*, a model plant for studying the molecular genetics of the *Rhizobium*-legume symbiosis. Plant Mol. Biol. Rep. **8,** 40–49.

Bhuvaneswari, T.V., Bhagwat, A.A., and Bauer, W.D. (1981). Transient susceptibility of root cells in four common legumes to nodulation by rhizobia. Plant Physiol. **68,** 1144–1149.

Bradley, D.J., Kjellbom, P., and Lamb, C.J. (1992). Elicitor- and wound-induced oxidative cross-linking of a proline-rich plant cell wall protein: A novel, rapid defense response. Cell **70,** 21–30.

Brown, J.W.S. (1986). A catalogue of splice junction and putative branch point sequences from plant introns. Nucl. Acids Res. **14,** 9549–9559.

Buffard, D., Breda, C., van Huystee, R.B., Asemota, O., Pierre, M., Ha, D.B.D., and Esnault, R. (1990). Molecular cloning of complementary DNAs encoding two cationic peroxidases from cultivated peanut cells. Proc. Natl. Acad. Sci. USA **87,** 8874–8878.

Caetano-Anollés, G., and Gresshoff, P.M. (1991). Alfalfa controls nodulation during the onset of *Rhizobium*-induced cortical cell division. Plant Physiol. **95,** 366–373.

Cordewener, J., Booij, H., van der Zandt, H., Van Engelen, F., van Kammen, A., and de Vries, S. (1991). Tunicamycin-inhibited carrot somatic embryogenesis can be restored by secreted cationic peroxidase isoenzymes. Planta **184,** 478–486.

Cox, K.H., and Goldberg, R.B. (1988). Analysis of plant gene expression. In Plant Molecular Biology: A Practical Approach, C.H. Shaw, ed (Oxford: IRL Press), pp. 1–34.

Criqui, M.C., Plesse, B., Durr, A., Marbach, J., Parmentier, Y., Jamet, E., and Fleck, J. (1992). Characterization of genes expressed in mesophyll protoplasts of *Nicotiana sylvestris* before the re-initiation of the DNA replication activity. Mech. Dev. **38,** 121–132.

de Billy, F., Barker, D.G., Gallusci, P., and Truchet, G. (1991). Leghaemoglobin gene transcription is triggered in a single cell layer in the indeterminate nitrogen-fixing root nodule of alfalfa. Plant J. **1,** 27–35.

Dudley, M.E., Jacobs, T.W., and Long, S.R. (1987). Microscopic studies of cell divisions induced in alfalfa roots by *Rhizobium meliloti*. Planta **171,** 289–301.

Feinberg, A.P., and Vogelstein, B. (1983). A technique for radiolabeling DNA restriction endonuclease fragments to high specific activity. Anal. Biochem. **132,** 6–13.

Fisher, R.F., and Long, S.R. (1992). *Rhizobium*-plant signal exchange. Nature **357,** 655–660.

Gallusci, P., Dedieu, A., Journet, E.P., Huguet, T., and Barker, D.G. (1991). Synchronous expression of leghaemoglobin genes in *Medicago truncatula* during nitrogen-fixing root nodule development and response to exogenously supplied nitrate. Plant Mol. Biol. **17,** 335–349.

Govers, F., Harmsen, H., Heidstra, R., Michielsen, P., Prins, M., van Kammen, A., and Bisseling, T. (1991). Characterization of the pea *ENOD12B* gene and expression analyses of the two *ENOD12* genes in nodule, stem and flower tissue. Mol. Gen. Genet. **228,** 160–166.

Horvath, B., Heidstra, R., Lados, M., Moerman, M., Spaink, H.P., Promé, J.-C., van Kammen, A., and Bisseling, T. (1993). Lipo-oligosaccharides of *Rhizobium* induce infection-related early nodulin gene expression in pea root hairs. Plant J. **4,** 727–733.

Journet, E.P., Pichon, M., Dedieu, A., de Billy, F., Truchet, G., and Barker, D.G. (1994). *Rhizobium meliloti* Nod factors elicit cell-specific transcription of the *ENOD12* gene in transgenic alfalfa. Plant J. **6,** 241–249.

Kieliszewski, M.J., and Lamport, D.T.A. (1994). Extensin: Repetitive motifs, functional sites, post-translational codes, and phylogeny. Plant J. **5,** 157–172.

Kondorosi, E., Gyruis, J., Schmidt, J., John, M., Duda, E., Hoffman, B., Schell, J., and Kondorosi, A. (1989). Positive and negative control of *nod* gene expression in *Rhizobium meliloti* is required for optimal nodulation. EMBO J. **8,** 1331–1340.

Kondorosi, E., Pierre, M., Cren, M., Haumann, U., Buire, M., Hoffman, B., Schell, J., and Kondorosi, A. (1991). Identification of NolR, a negative transacting factor controlling the *nod* regulon in *Rhizobium meliloti*. J. Mol. Biol. **222,** 885–896.

Kouchi, H., and Hata, S. (1993). Isolation and characterization of novel nodulin cDNAs representing genes expressed at early stages of soybean nodule development. Mol. Gen. Genet. **238,** 106–119.

Lerouge, P., Roche, P., Faucher, C., Maillet, F., Truchet, G., Prome, J.C., and Dénarié, J. (1990). Symbiotic host-specificity of *Rhizobium meliloti* is determined by a sulphated and acylated glucosamine oligosaccharide signal. Nature **344,** 781–784.

Lobler, M., and Hirsch, A.M. (1993). A gene that encodes a proline-rich nodulin with limited homology to PsENOD12 is expressed in the invasion zone of *Rhizobium meliloti*-induced alfalfa root nodules. Plant Physiol. **103,** 21–30.

Lullien, V., Barker, D.G., de Lajudie, P., and Huguet, T. (1987). Plant gene expression in effective and ineffective root nodules of alfalfa (*Medicago sativa*). Plant Mol. Biol. **9,** 469–478.

Lütcke, H.A., Chow, K.C., Mickel, F.S., Moss, K.A., Kern, H.F., and Scheele, G.A. (1987). Selection of AUG initiation codons differs in plants and animals. EMBO J. **6,** 43–48.

Mazza, G., and Welinder, K.G. (1980). Covalent structure of turnip peroxidase 7: Cyanogen bromide fragments, complete structure, and comparison to horseradish peroxidase C. Eur. J. Biochem. **108,** 481–489.

Perrey, R., Warskulat, U., and Wink, M. (1991). Molecular cloning of a *Lupinus polyphyllus* cDNA encoding a basic isoenzyme of cell suspension cultures. J. Plant Physiol. **137,** 537–540.

Pichon, M., Journet, E.-P., Dedieu, A., de Billy, F., Truchet, G., and Barker, D.G. (1992). *Rhizobium meliloti* elicits transient expression of the early nodulin gene *ENOD12* in the differentiating root epidermis of transgenic alfalfa. Plant Cell **4,** 1199–1211.

Rebmann, G., Hertig, C., Bull, J., Mauch, F., and Dudler, R. (1991). Cloning and sequencing of cDNAs encoding a pathogen-induced

putative peroxidase of wheat (*Triticum aestivum* L.). Plant Mol. Biol. **16,** 329–331.

Reimmann, C., Ringli, C., and Dudler, R. (1992). Complementary DNA cloning and sequence analysis of a pathogen-induced putative peroxidase from rice. Plant Physiol. **100,** 1611–1612.

Roche, P., Debellé, F., Maillet, F., Lerouge, P., Faucher, C., Truchet, G., Dénarié, J., and Prome, J. (1991). Molecular basis of symbiotic host specificity in *Rhizobium meliloti*: *nod*H and *nod*PQ genes encode the sulfation of lipo-oligosaccharide signals. Cell **67,** 1131–1143.

Rogers, S.O., and Bendich, A.J. (1988). Extraction of DNA from plant tissues. In Plant Molecular Biology Manual. (Dordecht, The Netherlands: Kulwer Academic Publishers), pp. 1–10.

Salzwedel, J.L., and Dazzo, F.B. (1993). pSym *nod* gene influence on elicitation of peroxidase activity from white clover and pea roots by rhizobia and their cell-free supernatants. Mol. Plant-Microbe Interact. **6,** 127–134.

Sambrook, J., Fritsch, E.F., and Maniatis, T. (1989). Molecular Cloning: A Laboratory Manual. (Cold Spring Harbor, NY: Cold Spring Harbor Laboratory Press).

Sanger, F., Nicklen, S., and Coulson, A.R. (1977). DNA sequencing with chain terminating inhibitors. Proc. Natl. Acad. Sci. USA **74,** 5463–5467.

Scheres, B., van Engelen, F., van der Knaap, E., van de Weil, C., van Kammen, A., and Bisseling, T. (1990a). Sequential induction of nodulin gene expression in the developing pea nodule. Plant Cell **2,** 687–700.

Scheres, B., van de Weil, C., Zalensky, A., Horvath, B., Spaink, H., van Eck, H., Zwartrkruis, F., Wolters, A., Gloudemans, T., van Kammen, A., and Bisseling, T. (1990b). The *ENOD12* gene product is involved in the infection process during the pea-*Rhizobium* interaction. Cell **60,** 281–294.

Shah, D.M., Hightower, R.C., and Meagher, R.B. (1982). Complete nucleotide sequence of a soybean actin gene. Proc. Natl. Acad. Sci. USA **79,** 1022–1026.

Sherrier, D.J., and VandenBosch, K.A. (1994). Localization of repetitive proline-rich proteins in the extracellular matrix of pea root nodules. Protoplasma, in press.

Thordal-Christensen, H., Brandt, J., Cho, B.H., Rasmussen, S.K., Gregersen, P.L., Smedegaard-Petersen, V., and Collinge, D.B. (1992). cDNA cloning and characterization of two barley peroxidase transcripts induced differentially by the powdery mildew fungus *Erysiphe graminis.* Physiol. Mol. Plant Pathol. **40,** 395–409.

Truchet, G., Roche, P., Lerouge, P., Vasse, J., Camut, S., de Billy, F., Prome, J.-C., and Dénarié, J. (1991). Sulphate lipo-oligosaccharide signals of *Rhizobium meliloti* elicit root nodule organogenesis in alfalfa. Nature **351,** 670–673.

Tyson, H. (1991). Relationships, derived from optimum alignments, among amino acid sequences of plant peroxidases. Can. J. Bot. **70,** 543–556.

Tyson, H. (1992). Relationship among amino acid sequences of animal, microbial and plant peroxidases. Theor. Appl. Genet. **84,** 643–655.

van Brussel, A.A.N., Bakhuizen, R., van Spronsen, P.C., Spaink, H.P., Tak, T., Lugtenberg, B.J.J., and Kijne, J.W. (1992). Induction of pre-infection thread structures in the leguminous host plant by mitogenic lipo-oligosaccharides of *Rhizobium.* Science **257,** 70–72.

VandenBosch, K.A., Bradley, D.J., Knox, J.P., Perotto, S., Butcher, G.W., and Brewin, N.J. (1989). Common components of the infection thread matrix and the intercellular space identified by immunocytochemical analysis of pea nodules and uninfected roots. EMBO J. **8,** 335–342.

van Engelen, F.A., and de Vries, S.C. (1992). Extracellular proteins in plant embryogenesis. Trends Genet. **8,** 66–70.

Vasse, J., de Billy, F., and Truchet, G. (1993). Abortion of infection during the *Rhizobium meliloti*-alfalfa symbiotic interaction is accompanied by a hypersensitive reaction. Plant J. **4,** 555–566.

Vincent, J.M. (1970). A Manual for the Practical Study of Root-Nodule Bacteria, IBP Handbook No. 15. (Oxford: Blackwell Scientific Press).

Vincent, J.M. (1980). Factors controlling the legume-*Rhizobium* symbiosis. In Nitrogen Fixation II, W.E. Newton and W.H. Orme-Johnson, eds (Baltimore, MD: University Park Press), pp. 103–109.

von Heijne, G. (1983). Patterns of amino acids near signal-sequence cleavage sites. Eur. J. Biochem. **133,** 17–21.

Wang, Z., and Brown, D.D. (1991). A gene expression screen. Proc. Natl. Acad. Sci. USA **88,** 11505–11509.

Wilson, R.C., Long, F., Maruoka, E.M., and Cooper, J.B. (1994). A new proline-rich early nodulin from *Medicago truncatula* is highly expressed in nodule meristematic cells. Plant Cell **6,** 1265–1275.

Yang, W., Katinakis, P., Hendriks, P., Smolders, A., de Vries, F., Spee, J., van Kammen, A., Bisseling, T., and Franssen, H. (1993). Characterization of GmENOD40, a gene showing novel patterns of cell-specific expression during soybean nodule development. Plant J. **3,** 573–585.

Zheng, X., and van Huystee, R.B. (1992). Peroxidase-regulated elongation of segments from peanut hypocotyls. Plant Sci. **81,** 47–56.